ARL-TN-1043 ● Oct 2020

DEVCOM ARMY RESEARCH LABORATORY

Experimental Procedure to Characterize the Effects of Filtering and Decoherence on Polarization Entangled Photons

by Daniel E Jones, Brian T Kirby, Gabriele Riccardi, Cristian Antonelli, and Michael Brodsky

NOTICES

Disclaimers

The findings in this report are not to be construed as an official Department of the Army position unless so designated by other authorized documents.

Citation of manufacturer's or trade names does not constitute an official endorsement or approval of the use thereof.

Destroy this report when it is no longer needed. Do not return it to the originator.

ARL-TN-1043 ● OCT 2020

Experimental Procedure to Characterize the Effects of Filtering and Decoherence on Polarization Entangled Photons

Daniel E Jones and Brian T Kirby
Computational and Information Sciences Directorate, CCDC Army Research Laboratory

Gabriele Riccardi and Cristian Antonelli
University of L'Aquila, Italy

Michael Brodsky
Computational and Information Sciences Directorate, CCDC Army Research Laboratory
US Military Academy

REPORT DOCUMENTATION PAGE

Form Approved
OMB No. 0704-0188

1. REPORT DATE *(DD-MM-YYYY)*	2. REPORT TYPE	3. DATES COVERED (From - To)
October 2020	Technical Note	1 October 2019–25 September 2020

4. TITLE AND SUBTITLE
Experimental Procedure to Characterize the Effects of Filtering and Decoherence on Polarization Entangled Photons

5a. CONTRACT NUMBER

5b. GRANT NUMBER

5c. PROGRAM ELEMENT NUMBER

6. AUTHOR(S)
Daniel E Jones, Brian T Kirby, Gabriele Riccardi, Cristian Antonelli, and Michael Brodsky

5d. PROJECT NUMBER

5e. TASK NUMBER

5f. WORK UNIT NUMBER

7. PERFORMING ORGANIZATION NAME(S) AND ADDRESS(ES)
CCDC Army Research Laboratory
ATTN: FCDD-RLC-NT
2800 Powder Mill Rd
Adelphi, MD 20783-1138

8. PERFORMING ORGANIZATION REPORT NUMBER
ARL-TN-1043

9. SPONSORING/MONITORING AGENCY NAME(S) AND ADDRESS(ES)

10. SPONSOR/MONITOR'S ACRONYM(S)

11. SPONSOR/MONITOR'S REPORT NUMBER(S)

12. DISTRIBUTION/AVAILABILITY STATEMENT
Approved for public release; distribution is unlimited.

13. SUPPLEMENTARY NOTES
ORCID IDs: Daniel E Jones, 0000-0002-9854-5767; Brian T Kirby, 0000-0002-2698-9887

14. ABSTRACT
We transmitted one photon of an entangled pair through a fiber channel that includes decoherence and partial filtering elements. We then demonstrated that a local filter could be applied to the other photon of the entangled pair in order to maximize the mutual quantum information between the photons. We showed that the relative orientation of the decoherence and filtering elements can be altered to emulate two types of noise, bit-flip noise and phase-flip noise, which are common to quantum channels. This note describes the exact experimental procedure that was followed to apply decoherence and filtering via polarization mode dispersion and polarization-dependent loss, respectively, to demonstrate our results.

15. SUBJECT TERMS
quantum entanglement, quantum networks, quantum communication, quantum information, quantum channels, polarization mode dispersion, PMD, polarization-dependent loss, PDL

16. SECURITY CLASSIFICATION OF:			17. LIMITATION OF ABSTRACT	18. NUMBER OF PAGES	19a. NAME OF RESPONSIBLE PERSON
a. REPORT	b. ABSTRACT	c. THIS PAGE			Daniel E Jones
Unclassified	Unclassified	Unclassified	UU	15	19b. TELEPHONE NUMBER (Include area code) (301) 394-0503

Contents

List of Figures

1. Introduction

In our recent work,[1] we transmitted one photon of an entangled pair through a fiber channel that included decoherence and partial filtering elements. We then demonstrated that a local filter could be applied to the other photon of the entangled pair in order to maximize the mutual quantum information between the photons. We showed that the relative orientation of the decoherence and filtering elements can be altered to emulate two types of noise, bit-flip noise and phase-flip noise, which are common to quantum channels. Although only a small amount of mutual information can be recovered in the presence of bit-flip noise, all mutual information can be recovered in the presence of phase-flip noise.

To implement the decoherence and local filter elements, we used polarization mode dispersion (PMD) and polarization-dependent loss (PDL) emulators. PMD[2–9] and PDL[10–19] are thoroughly researched properties of optical fibers. Randomly varying birefringence accumulates along the length of optical fibers and results in PMD, the phenomenon in which an input pulse separates into two orthogonally polarized components with a relative delay.[2,3] PDL is a common effect in fiber-optic components in which one polarization mode experiences more loss compared to the other. PMD and PDL are the primary polarization decoherence and filtering mechanisms in optical fibers.[1,18–22] Thus, applying PMD and PDL emulators to the fiber channels traversed by the entangled photons offers a practical implementation of the decoherence and filtering that occurs when distributing entangled photons over the existing telecom infrastructure. This note describes the exact experimental procedure that was followed to apply decoherence and filtering via PMD and PDL, respectively, to demonstrate the results shown in Jones et al.[1]

2. Experimental Setup

We used the setup shown in Fig. 1 to physically realize the experiment depicted in Fig. 1a of Jones et al.[1] The decoherence/birefringence $\vec{\beta}_A$ is applied via the unit designated PMDA, which consists of a polarization controller (PCA1) and a PDL/PMD emulator, which applies variable PDL and a fixed differential group delay (DGD) of τ = 6.6 ps. The mode filter inherent to channel A ($\vec{\gamma}_A$) and the network operator's filter ($\vec{\gamma}_B$) are each realized with the combination of a polarization controller and a variable PDL emulator, denoted PDLA and PDLB in Fig. 1. The PDL of all emulators is fully tunable in magnitude and direction. Furthermore, our setup is based on an entanglement distribution system comprising an entangled photon-pair source (EPS), which distributes entangled photons to two

detector stations (DSs), each consisting of a polarization analyzer (PA) and an indium gallium arsenide single-photon detector (SPD).[23]

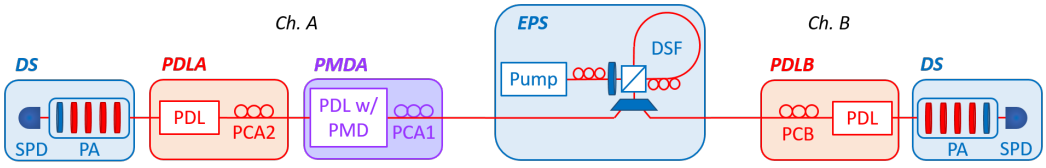

Fig. 1 Experiment schematics: (left to right) DS (SPD with a PA consisting of a polarizer [blue] and several waveplates [red]), PDL emulator (with polarization controller PCA2), PDL with PMD (PDL/PMD emulator that applies a DGD of τ = 6.6 ps, with polarization controller PCA1), EPS (pump with a dispersion-shifted fiber [DSF]), PDL emulator (polarization controller PCB), and DS (a PA consisting of several waveplates [red] and a polarizer [blue] and an SPD)

Signal and idler photons are generated by the EPS via four-wave mixing[24] using a 50-MHz pulsed fiber laser with a center wavelength of 1552.52 nm to pump a DSF. The signal and idler are entangled in polarization by arranging the DSF in a Sagnac loop with a polarization beam splitter. Photons with a temporal duration of about 15 ps are output by the EPS, after a WDM demultiplexer separates the photons spectrally into 100-GHz-spaced International Telecommunication Union (ITU) outputs after the Sagnac loop.[25] Photons in ITU channel 28 (1554.94 nm) are sent to channel A, and those in ITU channel 34 (1550.12 nm) are sent to channel B. The average number of pairs per pump pulse output by the EPS is approximately $\mu = 0.001 - 0.1$.[26,27] The detectors are gated and have a detection efficiency of $\eta \sim 20\%$ and a dark count probability of approximately 4×10^{-5} per gate. Automated software controls the PAs and SPDs to perform full polarization state tomography to determine the density matrix at the two DSs.

3. Mitigating Source Misalignment

Our EPS typically outputs a slightly misaligned entangled state that is equivalent to a $|\varphi^+\rangle$ Bell state, which experiences approximately 1.4 dB of PDL in one channel.[18] To compensate for the effect of this "source PDL", the magnitude of the PDL applied by the first emulator PMDA was set to 1.4 dB. The orientation of PCA1 was then adjusted until the optimum orientation of PCA1 was found by performing quantum state tomography and monitoring the measured density matrix. The orientation of PCA1 was then fixed, that is, it always remained opposite of the direction of the "source PDL". Using this method, we were able to reduce the aggregate "source PDL" from 1.4 dB to 0.1 dB (as seen in Fig. 1 and the left-most plot of Fig. 2d in Jones et al.).[1]

4. Applying PDL in Channel A

The PDL and PMD in channel A are further controlled by PMDA and PDLA. PMDA applies PMD and PDL in a collinear fashion. Using PMDA, we applied a DGD of τ = 6.6 ps. Then, we applied variable PDL to channel A using PDLA. Our experiment investigated the relative alignment of the PMD and PDL vectors of channel A. Next, we describe the alignment procedure.

To align the total PDL of the entire channel A ($\vec{P}_A$) relative to the PMD applied via PMDA, the PDL applied by PMDA was temporarily increased to approximately 5 dB to set a reference signal in the same direction as the PMD applied by PMDA. This allowed us to align the PDL applied by PDLA relative to the reference signal. To set up the bit-flip case, we aligned PDLA such that the PMD and PDL of channel A were orthogonal. For this, PCA2 was continuously adjusted until the total PDL measured from the continuously monitored density matrix was equal to the aggregate PDL of the reference signal and an orthogonal PDLA vector. On the other hand, to set up the phase-flip case, PCA2 was rotated such that the total PDL of the density matrix was minimized, resulting in collinear PDL and PMD in channel A. After aligning PDLA (in both cases), the magnitude of the PDL applied by PMDA was set back to 1.4 dB, thus canceling the "source PDL".

Finally, state tomography was performed and the mutual information was calculated from the measured density matrices using the expression $S(A:B) = S(A) + S(B) - S(AB)$, where $S(AB)$ is the von Neumann entropy of the entire two-qubit state (ρ) measured by tomography, $S(\rho) = -\mathrm{Tr}\{\rho \ln[\rho]\}$, and $S(A)$, $S(B)$ are the marginal entropies.

5. Applying PDL in Channel B

The emulator included in PDLB controls the magnitude of PDLB ($\vec{P}_B$). We first set the magnitude (P_B) of PDLB as explained here and then set its orientation by adjusting the polarization controller PCB until the entanglement was maximized. The feedback parameter was the concurrence that was calculated from the measured density matrices.

For the bit-flip experimental scenario, P_B was set to two different values for each value of P_A. It was first set equal to P_A. Next, it was decreased to the optimum value given by $P_B^{\mathrm{opt}} = \tanh^{-1}(C\ \tanh(\gamma_A)) \times (20\log_{10} e)$.[1] For the phase-flip scenario, P_B was only set equal to the magnitude of the PDL in channel A ($P_B = P_A$). This procedure was repeated for all values of PDL in channel A (P_A). We chose the range of PDLA magnitudes to be $P_A = 5.70 - 7.65$ dB ($\gamma_A = 0.656 - 0.880$) for the bit-flip data. For the phase-flip data, the range was $P_A = 3.42 - 7.97$ dB

($\gamma_A = 0.394 - 0.918$). For the PDLA magnitudes $P_A = 7.12, 7.44,$ and 7.55 dB ($\gamma_A = 0.820, 0.857, 0.869$), an additional measurement was performed with P_B set to a value of $P_B \approx P_B^{\text{opt}}/2$ to better characterize the amount of mutual information recovered as a function of P_B.

Every data point in Fig. 2 of Jones et al.[1] is the average mutual information over several consecutive tomography measurements. The error bars represent the standard deviation of these consecutive measurements. Each quantum state tomography was performed over 100 million detector gates per measurement. Given the 50-MHz pump laser repetition rate (20-ns period), 36 measurement settings per tomography, and approximately 5 s required to calculate the density matrix via maximum-likelihood estimation, each tomography took approximately 80 s.

6. Conclusion

This note describes the exact experimental procedure to apply PMD and PDL to polarization entangled photons in order to emulate two types of noise common to quantum channels and recover the mutual information lost due to these types of noise. By following these procedures, one can demonstrate the recovery of all mutual information lost due to phase-flip noise via local filtering (i.e., application of PDL in channel B). However, only a small amount of the mutual information can be recovered for the case of bit-flip noise.

7. References

1. Jones DE, Kirby BT, Riccardi G, Antonelli C, Brodsky M. Exploring classical correlations in noise to recover quantum information using local filtering. New J Phys. 2020;22:073037.

2. Gordon J, Kogelnik H. PMD fundamentals: polarization mode dispersion in optical fibers. Proc Natl Acad Sci. 2000;97(9):4541.

3. Brodsky M, Frigo NJ, Tur M. Optics and photonics. In: Kaminow IP, Li T, Willner AE, editors. Optical fiber telecommunications A. 5th ed. Burlington (MA): Academic Press; 2008. p. 605–669.

4. Brodsky M, Magill PD, Frigo NJ. Evidence for parametric dependence of PMD on temperature in installed 0.05 ps/km$^{1/2}$ fiber. European Conference on Optical Communication. 2002;4:1–2.

5. Boroditsky M, Brodsky M, Frigo NJ, Magill P, Raddatz L. In-service measurements of polarization mode dispersion and correlation to bit-error rate. IEEE Photon Technol Lett. 2003;15:572–574.

6. Brodsky M, Boroditsky M, Magill PD, Frigo NJ, Tur M. Physical mechanism for polarization mode dispersion temporal dynamics. European Conference on Optical Communication. 2004;3:306–309.

7. Mecozzi A, Antonelli C, Boroditsky M, Brodsky M. Characterization of the time dependence of polarization mode dispersion. Opt Lett. 2004;29:2599–2601.

8. Antonelli C, Mecozzi A, Cornick K, Brodsky M, Boroditsky M. PMD-induced penalty statistics in fiber links. IEEE Photonics Technol Lett. 2005;17:1013–2015.

9. Brodsky M, Boroditsky M, Magill P, Frigo N, Tur M. Persistence of spectral variations in DGD statistics. Opt Express. 2005 May;13(11):4090–4095.

10. Gisin N. Statistics of polarization dependent losses. Opt Comm. 1995 Feb;114(5–6):399–405.

11. Mecozzi A, Shtaif M. The statistics of polarization-dependent loss in optical communication systems. IEEE Photon Technol Lett. 2002;14(3):313–315.

12. Galtarossa A, Palmieri L. The exact statistics of polarization-dependent loss in fiber-optic links. IEEE Photon Technol Lett. 2003;15(1):57–59.

13. Vinegoni C, Karlsson M, Petersson M, Sunnerud H. Statistics of polarization-dependent loss in a recirculating loop. J Lightwave Technol. 2004;22:968–976.

14. Liboiron-Ladouceur O, Bergman K, Boroditsky M, Brodsky M. Polarization-dependent gain in SOA-based optical multistage interconnection networks. J Lightwave Technol. 2006;24(11):3959–3967.

15. Shtaif M, Rosenberg O. Polarization-dependent loss as a waveform-distorting mechanism and its effect on fiber-optic systems. J Light Technol. 2005;23(2):923.

16. Shtaif M. Performance degradation in coherent polarization multiplexed systems as a result of polarization dependent loss. Opt Express. 2008;16(18):13918–32.

17. Medic M, Kumar P. Effects of polarization-dependent loss and fiber birefringence on photon-pair entanglement in fiber-optic channels. Optical Society of America, Photonic Applied System Technology Conference; 2007; Baltimore, MD. p. JTuA16.

18. Jones DE, Kirby BT, Brodsky M. Tuning quantum channels to maximize polarization entanglement for telecom photon pairs. NPJ Quantum Inf. 2018;4(1):1–7.

19. Kirby BT, Jones DE, Brodsky M. Effect of polarization dependent loss on the quality of transmitted polarization entanglement. J Light Technol. 2019;37(1):95–102.

20. Antonelli C, Shtaif M, Brodsky M. Sudden death of entanglement induced by polarization mode dispersion. Phys Rev Lett. 2011;106:080404.

21. Brodsky M, George EC, Antonelli C, Shtaif M. Loss of polarization entanglement in a fiber-optic system with polarization mode dispersion in one optical path. Opt Lett. 2011;36(1):43–45.

22. Shtaif M, Antonelli C, Brodsky M. Nonlocal compensation of polarization mode dispersion in the transmission of polarization entangled photons. Opt Express. 2011 Jan;19(3):1728–33.

23. Quantum optical instrumentation. Evanston (IL): NuCrypt; 2017 [accessed 2020 Sep 25]. http://nucrypt.net/quantum-optical-instrumentation.html.

24. Fiorentino M, Voss PL, Sharping JE, Kumar P. All-fiber photon-pair source for quantum communications. IEEE Photon Technol Lett. 2002;14(7):983–985.

25. Wang SX, Kanter GS. Robust multiwavelength all-fiber source of polarization-entangled photons with built-in analyzer alignment signal. IEEE J Sel Top Quantum Electron. 2009;15(6):1733–1740.

26. Jones DE, Kirby BT, Brodsky M. Joint characterization of two single photon detectors with a fiber-based source of entangled photon pairs. Frontiers in Optics; 2017 Sep 18–21; Washington, DC. Optical Society of America. p. JW4A.37.

27. Jones DE, Kirby BT, Brodsky M. In-situ calibration of fiber-optics entangled photon distribution system. IEEE Photonics Society. Summer Topical Meeting Series; 2017; San Juan, Puerto Rico. IEEE. p. 123–124.

List of Symbols, Abbreviations, and Acronyms

ARL	Army Research Laboratory
CCDC	US Army Combat Capabilities Development Command
DGD	differential group delay
DS	detector station
DSF	dispersion-shifted fiber
EPS	entangled photon-pair source
ITU	International Telecommunication Union
PA	polarization analyzer
PDL	polarization-dependent loss
PMD	polarization mode dispersion
SPD	single-photon detector

1 (PDF)	DEFENSE TECHNICAL INFORMATION CTR DTIC OCA
1 (PDF)	CCDC ARL FCDD RLD DCI TECH LIB
3 (PDF)	CCDC ARL FCDD RLC NT M BRODSKY DE JONES BT KIRBY